Materials Science Forum Vols. 378-381 (2001) pp. 771-776

Magnetic Cation Distribution in a Nanocrystalline Fe_3O_4 Spinel

Z. Somogyvári[1], E. Sváb[1], Gy. Mészáros[1], K. Krezhov[2], P. Konstantinov[2], T. Ungár[3] and J. Gubicza[3]

[1] Research Institute for Solid State Physics and Optics, Hungarian Academy of Sciences, PO Box 49, HU-1525 Budapest, Hungary

[2] Institute for Nuclear Research and Nuclear Energy, Bulgarian Academy of Sciences, 72 Tzarigradsko Chaussee, BU-1784 Sofia, Bulgaria

[3] Department for General Physics, Loránd Eötvös University, PO Box 32, HU-1518 Budapest, Hungary

Keywords: Cation Distribution, Line Profile Analysis, Magnetic Sublattice, Magnetite, Nano-Size, Neutron Diffraction, Spinel

Abstract. Neutron diffraction study of nanostructured magnetite was performed at room temperature. The actual grain-size was determined from evaluation of X-ray diffraction profiles by the modified Williamson-Hall plot. The atomic structure parameters and the sublattice magnetic moments were determined using the Rietveld refinement of the neutron diffraction spectra. The sublattice magnetization at the octahedral sites decreases with decreasing grain-size, while it remains practically constant at the tetrahedral sites.

1. Introduction

The early studies of magnetite Fe_3O_4 already [1] have established that it is a mixed valency compound. Below the Curie temperature of approximately 770 K down to the Verwey transition temperature of about 119 K [2], at which a disorder-order phase transition to a structure with lower symmetry takes place, its crystal structure is that of an inverse cubic spinel. The tetrahedral A sites are occupied solely by trivalent Fe ions and the octahedral B sites are occupied at random by Fe^{2+} and Fe^{3+} ions in equal numbers. The diffracted neutron intensities of powdered [1] or single crystalline [3] magnetite were in good agreement with the Néel's model of collinear ferrimagnetism.

On the other hand, there is a steady growth of interest in nanostructured materials during the last decade, stimulated by recent advances in material synthesis and characterisation techniques [4]. These materials were found to exhibit many unique and interesting physical and chemical properties with a number of potential technological applications. Examples are ferrofluids, particulate magnetic recording media, catalysts etc. Evidence is accumulated that magnetic nanocrystalline powders show unusual magnetic behaviour when compared to the bulk materials. It is mostly due to surface/interface effects, including symmetry breaking, electronic environment/charge transfer, and magnetic interactions. Furthermore, because of the high surface area/volume ratio they represent surface and interfacial material in bulk quantities, thus a new magnetism may develop.

It has been shown recently [5] that the microwave absorption of powder pellets of Fe_3O_4 nano-sized material prepared by the chemical coprecipitation method improves and the resonance frequency can be regulated, i.e. shifted, depending on the grain size. A possible reason for this could be that the cation distribution and associated sublattice magnetic moments, which proved to be of high importance for the electric and magnetic properties of oxide ferrites, might be changed as compared with the magnetite prepared by the conventional ceramic technique.

The aim of the present study was to investigate the effect of nanometer scale grain sizes on the cation distribution and magnetic moments ordering in such nanocrystalline magnetite. Here is to be noted that evidence on magnetic properties of iron oxides in small particle form is customary obtained by macroscopic magnetic methods and Mössbauer spectroscopy is used most frequently

for determination of magnetic structural changes [4]. The application of neutron scattering techniques is not so common but yielded valuable information on $ZnFe_2O_4$ material of nanometer-sized crystallites [6].

2. Experimental details

2.1. Sample preparation

Four Fe_3O_4 powder samples of different grain-size were investigated (see Table 1). Two specimens of nano-sized (d=17 and 28 nm) and one of fine-grained (d=640 nm) material were produced by the chemical coprecipitation procedure described by Tronc and co-workers [7]. In our case thoroughly mixed aqueous solutions of $FeCl_2.4H_2O$ and $NaNO_2$ taken in suitable concentration ratios were co-precipitated at room temperature in strongly alkaline medium (pH>10) by adding sodium base. The resulting precipitate was washed with deionized water and then dried at a temperature of about 80 °C. As shown by Nedkov et al [8], the grain-size of the deep black material may be controlled to great extent since it is dependent on the actual pH value of the medium where the co-precipitation process takes place. The fourth nano-sized sample of d=54 nm was from a commercial Fe_3O_4 material purchased from Johnson-Mathey Ltd.

2.2. X-ray diffraction

The unit cell parameter of the specimens has been evaluated from X-ray diffraction refinement of the patterns taken at ambient temperature by means of a Philips Xpert diffractometer using CuK_α radiation.

In addition, high resolution X-ray diffraction profile analysis was performed for determination of the average grain-sizes of the specimens. The diffraction profiles were measured by a special double crystal diffractometer with negligible instrumental broadening [9].

2.3. Neutron diffraction

Room temperature neutron diffraction spectra in the range from 8 to 95 degrees in 2Θ scattering angle were collected on the medium resolution PSD neutron diffractometer installed at the 10 MW steady state research reactor in Budapest [10]. The monochromated neutron wavelength was λ=0.1059 nm ($\lambda/2$ contamination less than 0.4%). The fine powder specimens were filled in cylindrical vanadium sample holder of 0.07 mm wall thickness, 5 mm diameter and 20 mm height. Before evaluation the raw data were corrected for instrumental background.

3. Data evaluation

3.1. Evaluation of the X-ray diffraction profiles by the modified Williamson-Hall plot

It has been shown recently that anisotropic strain-broadening of the diffraction profiles can be well accounted for by the dislocation model of the mean square strain [11]. The model takes into account that the contrast caused by dislocations depends on the relative directions of the line and Burgers vectors of the dislocations and the diffraction vector, respectively. Anisotropic contrast can thus be summarised in contrast factors, C, which can be calculated numerically on the basis of the crystallography of dislocations and the elastic constants of the crystal [12-15]. By appropriate determination of the type of dislocations and Burgers vectors present in the crystal, the average contrast factors, C, for the different Bragg reflections can be determined. Using the average contrast factors in the *modified* Williamson-Hall plot, the integral breadths ΔK of diffraction profiles can be given in the following form [11,16]:

$$\Delta K = 1 / d + \alpha (K\overline{C}^{1/2})^2 + O(K\overline{C}^{1/2})^4 , \quad (1)$$

where d is a size parameter, α is a constant depending on the effective outer cut-off radius, the Burgers vector and the density of dislocations. In the present case d is close to the arithmetic average of the crystallite size assuming log-normal size distribution and spherical crystallites. K is the length of the diffraction vector: $K=2\sin\theta/\lambda$, where θ is the diffraction angle and λ is the wavelength of X-rays. O stands for higher order terms in $K^4\overline{C}^2$. $\overline{C}$ is the contrast factor of dislocations depending on the relative positions of the diffraction vector and the Burgers and line vectors of the dislocations, the character of dislocations and the elastic constants of the crystal [12-15]. It has been shown that the average dislocation contrast factors in an untextured cubic polycrystal are a simple function of the invariants of the fourth order polynomials of Miller indices [17]:

$$\overline{C} = \overline{C}_{h00} (1-qH^2) , \quad (2)$$

where $\overline{C}_{h00}$ is the average dislocation contrast factor for the $h00$ reflections, q is a parameter depending on the elastic constants of the crystal and the edge or screw character of dislocations and $H^2=(h^2k^2+h^2l^2+k^2l^2)/(h^2+k^2+l^2)^2$ [7,9]. The size parameter, d, is obtained from the intercept at $K\overline{C}^{1/2}=0$ of a smooth curve according Eq. 1.

3.2. Structure refinement

The neutron diffraction patterns (corrected for absorption effects according to pin-hole measured transmission) were refined by the Rietveld method using the program package Fullprof [18]. For the structure factor calculations the origin of the unit cell was taken at the centre of symmetry $\bar{3}m$, the tetrahedral, octahedral and oxygen sites being in 8(a), 16(d) and 32(e) of the space group $Fd\bar{3}m$, respectively. Beside the instrumental parameters describing zero point shift, peak shape, peak asymmetry and angular dependence of the full width at half maximum (FWHM), also the oxygen positional parameter and the average magnetic moments of the tetrahedral and octahedral sublattices were determined. The background polynomial parameters and isotropic temperature factors of oxygen and the effective scatterers on A and B sites were refined simultaneously with the other structural parameters.

Several magnetic structure models were tested against the neutron scattering data. The results of the refinements were compared with the Néel's model of collinear ferrimagnetic ordering taken as a basis.

4. Results and Discussion

Figure 1 illustrates the modified Williamson-Hall plot of the integral breadth according to Eq. (1) for one of the specimens. The intercept at $K\overline{C}^{1/2}=0$ gives d = 28 nm. The values of d for the rest specimens investigated were 17, 54, and 640 nm.

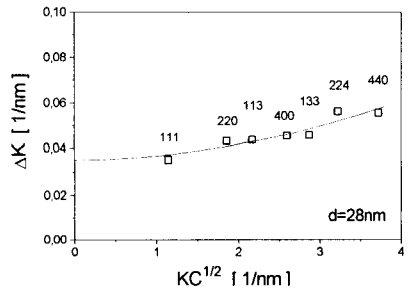

Fig. 1: The modified Williamson-Hall plot of integral breadth for Fe_3O_4 specimen of d=28 nm grain-size. The Miller indices of the reflections are also indicated.

The neutron diffraction spectra for the four samples are shown in Fig. 2. The Johnson-Matthey and 640 nm Fe_3O_4 samples were found to contain traces of hematite (α-Fe_2O_3, $R\bar{3}c$) as a second phase, less than 3 % and 8 %, correspondingly. Both neutron and X-ray analysis indicated that the rest two specimens were essentially pure Fe_3O_4 phase.

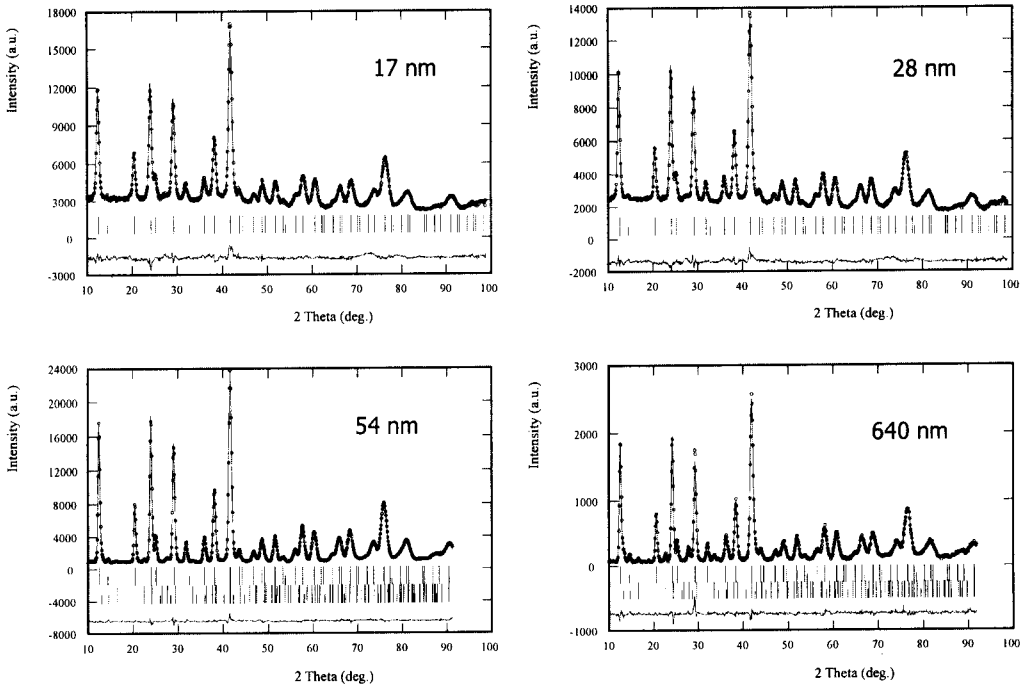

Fig. 2: Neutron diffraction patterns and Rietveld refinement of different grain-sized Fe_3O_4 specimens (d=17, 28, 54 and 640 nm). The tick marks (from top to bottom) denote the positions of nuclear and magnetic Bragg reflections corresponding to Fe_3O_4 ($Fd\bar{3}m$) and to α-Fe_2O_3 ($R\bar{3}c$) phases.

The inspection of the recorded patterns has shown that the difference in the experimental structure factors of corresponding Bragg reflections is small. It is more distinct in the lower angular part of the patterns indicating a slight change in the magnetic contribution. Also, a large diffuse contribution to the scattered intensity was observed in the case of the nanocrystalline samples of d=17 nm and 28 nm.

The simple model for ferrimagnetic arrangement described the spectra reasonably well, as can be seen in Fig. 2. Isotropic magnetic form factors of Fe^{2+} and Fe^{3+} ions were used.

The results for the unit cell parameters calculated from the X-ray data and the refined crystal and magnetic structural parameters obtained from the neutron diffraction spectra are summarized in Table 1.

Table 1. Structural parameters of Fe_3O_4: grain-size, d, unit cell parameter, a_0, oxygen positional parameter, u, effective magnetic moments on the A sites, m_A, and the B sites, m_B, and calculated magnetic moment M per formula unit.

d (nm)	a_0 (Å)	u	Sublattice magnetic moments		M (μ_B)
			m_A (μ_B)	m_B (μ_B)	
17	8.358(1)	0.2555(1)	4.15(9)	-3.39(6)	2.6(2)
28	8.373(1)	0.2551(1)	4.03(7)	-3.55(5)	3.1(2)
54	8.388(1)	0.2547(1)	4.01(4)	-3.61(3)	3.2(2)
640	8.395(1)	0.2544(2)	3.99(8)	-3.66(5)	3.3(2)

The lattice constant for the fine-grain specimen (d=640 nm) is in good agreement with the values shown in the survey on microcrystalline magnetite [19], while for the nano-sized materials its value is decreasing. Also, the oxygen parameter slightly decreases with increasing grain-size. Here, we should note that similar behaviour of these structural parameters was established by the neutron diffraction analysis of 9 nm grain-sized $ZnFe_2O_4$ [6]. Moreover, the nanostructured $ZnFe_2O_4$ was found to order ferromagnetically already at T_c approx. 500 K and an unexpected small value was refined for the ordered moment values of 2.5 μ_B per Fe at 4.2 K.

In our case, as seen from Table 1, the refined values of sublattice magnetization show a trend for increase of m_B with growing grain-size, while m_A remains practically constant within the error limits. In any case it is clear that there is a reduction of the estimated magnetic moment per formula unit, M, exceeding 20% as compared to the room temperature value of 4.1 μ_B known for Fe_3O_4 from the literature [1].

The last result is in overall consistence with our preliminary measurements of saturation magnetization. It is not surprising because the magnetization of ferromagnetic oxide small particles is generally observed to be less than that of the bulk. In several such cases the Mössbauer spectra in strong applied fields indicate non-collinearity in magnetic structure. Another point discussed broadly in the literature is that the surface of magnetic small particles exhibits some properties that are different from the bulk. The particle is viewed as consisting of an inner core and an outer shell. In case of small particles with a non-collinear magnetic moments arrangement the symmetry breaking in superexchange interactions near the surface might contribute to the magnetic moment reduction. Although the presence of spin canting will lead to reduced magnetization still some additional factors seem to be required to account for the low magnetization observed. The surface effects on magnetism are a research field of increasing importance. The first topographic and magnetic-sensitive measurement by scanning tunnelling microscope with magnetic probe tips carried out on the surface of natural single crystals of magnetite at room temperature showed magnetic moments ordering with 12 Å periodicity in rows attributed to the octahedral sites [20]. Such an ordering is observed by methods sensitive to long- range order only below the charge order-disorder (Verwey) transition, which is well below room temperature. On the other hand this kind of relatively short-range orderings should result in the increase of the diffuse 'background' in powder diffraction patterns.

The presence of vacancies at the iron sites in the nano-sized specimens may also lead to the observed decreased value of the lattice constant and to the decrease of the average magnetic

moment. It is well known from the literature that maghemite (γ-Fe_2O_3) has a similar spinel-type structure like magnetite, but with ordered vacancies at the octahedral Fe-sites [21]. In our case, no superstructure lines were observed in the diffraction pattern. Anyhow, the presence of a random distribution of vacancies cannot be excluded. We have tried several models, but the measured intensity data proved not to be of sufficient quality to allow for some of the other structural models tested to be unambiguously proved. The simultaneous determination of sublattice magnetic moments and site occupancies yielded large correlations between the estimated parameters. In order to explain the findings summarized in Table 1, further model calculations are in progress. Modelling of the large diffuse scattering of the nano-sized specimens of d=17 and 28 nm is also in progress by the recently developed RMCPOW algorithm [22].

Acknowledgements

We are grateful to Dr. L. F. Kiss for magnetic measurements and to Dr. L. Kőszegi for helpful discussions. The financial support by the Hungarian Scientific Research Fund, OTKA, Grant Nos. T-29402, D-29339 and T-031786, by the Bulgarian National Fund for Science under contract F-816 and by the EC HPRI-CT-1999-00099 is gratefully acknowledged.

References

[1] C. Shull, E. Wollan, W. Koeler, Phys. Rev. 84 (1951), p. 912.
[2] R. Valenzuela, Magnetic ceramics, Cambridge University Press, Cambridge, (1994).
[3] W. Hamilton, Phys. Rev. 110 (1958), p. 1050.
[4] A. Hernando, Nanomagnetism, Kluwer Academic Publishers, Dordrecht, (1993).
[5] I. Nedkov et al – IEEE Trans. Magn. Magn. Mat. (1994)
[6] W. Schafer, W. Kockelmann, A. Kirfel, W. Potzel, F. Burghart, G. Kalvius, A. Martin, W. Kacymarek, S. Campbell, Mater. Sci. Forum 321-324 (2000), p. 802.
[7] J. P. Jolivet, C.Chaneac, P. Prene, L. Vaysieres, E. Tronc, J. Phys. IV (France) **7** (1997) C1-573.
[8] I. Nedkov, T. Merodijska, L. Milenova, T. Koutzarova, JMMM 211 (2000), p. 296.
[9] T. Ungár, S. Ott, P. Sanders, A. Borbély and J. R. Weertman, Acta Mater. 46 (1998), p. 3693.
[10] E. Sváb, F. Deák, D. Mészáros, Mater. Sci. Forum., 228-231, (1996), p. 247.
[11] T. Ungár and A. Borbély, Appl. Phys. Lett. 69 (1996), p. 3173.
[12] M. Wilkens, phys. stat. sol. (a) 104 (1987) K1.
[13] P. Klimanek and R. Kuzel Jr., J. Appl. Cryst. 21 (1988), p. 59.
[14] R. Kuzel Jr. and P. Klimanek, J. Appl. Cryst. 21 (1988), p. 363.
[15] T. Ungár, I. Dragomir, Á. Révész and A. Borbély, J. Appl. Cryst. 32 (1999), p. 992.
[16] T. Ungár, J. Gubicza, G. Ribárik and A. Borbély, in preparation
[17] T. Ungár and G. Tichy, phys. stat. sol. (a) 171 (1999), p. 425.
[18] J. Rodríguez-Carvajal, Fullprof
[19] H. St. C. O'Neill, W. Dollase, Phys. Chem. Minerals 20 (1994), p. 541.
[20] R. Wiesendanger, , Science 255, (1992), p. 583.
[21] A. N. Shmakov, G. N. Kryukova, S. V. Tsybulya, A. L. Chuvilin, L. P. Solovyeva, J. Appl. Cryst. 28 (1995), p. 141.
[22] A. Mellergard, R.L. McGreevy, Acta Cryst. A55 (1999), p. 783.

Corresponding author: Z. Somogyvári e-mail: zs@szfki.hu Fax:+36-1-3922589